

# Overview of RBF NN and Antenna Systems

MAJA SAREVSKA

AUE-FON, Kiro Gligorov 5, 1000 Skopje, NORTH MACEDONIA

**Abstract:** This paper presents the application of Radial Basis Function neural network in antenna array systems and in the estimation of polarization rotation estimation in the ionosphere. Radial Basis Function neural network is used as it satisfies both universal and best approximation property. We present the architecture of the network, as part of the total system. Presented results show low mean error values and very good match between the referent values and gained one, which shows the successfulness of the particular neural network.

**Keywords:** Antenna Array, Array Factor, Neural Network, Radial Basis Function Neural Network

Received: May 19, 2021. Revised: July 2, 2022. Accepted: August 5, 2022. Published: September 14, 2022.

## 1. Introduction

**T**HE artificial neural networks theory and design advanced significantly in the last decades. Also, signal processing is the field where much progress has been achieved. Neural Networks (NN) are highly suited for solving difficult signal processing problems, mostly because of their non-linear nature, their universal approximation property and their ability to learn from environment in both supervised and unsupervised ways..

A network of many simple processors (units, nodes, or neurons) presents the NN, where all these units are interconnected with unidirectional communication channels (connections) labeled with numerical data, also having a small amount of local memory [1]. For the NN we can think as a black box that has certain input and produces certain outputs. The NN structure and neurons models determine the functionality of this black box.

It is interesting to note that NN resembles the brain in the following two aspects:

- A learning process provides the NN to acquire a knowledge
- Synaptic weights presented by interneuron connection are storing that knowledge

The one of most exciting properties of NNs is their functional approximation capability that makes them suitable for applications in signal processing, control, communication channel equalization, pattern recognition and system identification. The approximation capabilities of various types of multilayered feedforward architectures have been investigated since 1990's with much interest. Actually a feedforward NN may be seen as a rule of computing the output values of the neurons in the  $i$ th layer from the values of the

outputs of the  $(i-1)$ th layer, that actually present a mapping from the input space  $R^n$  to an output space  $R^n$ .

The Stone-Weierstrass theorem is effective analytical tool for function approximation analyses [2]. The relationship between the Kolmogorov's theorem and approximation principle of the feedforward networks was found in 1980's. This theorem states that a continuous multivariable function may be expressed, on a compact domain, in terms of sums of compositions on single variable functions. It was shown that NNs with at least one hidden layer are capable of approximating continuous function if the activation functions of the hidden neurons are differentiable.

A suitable candidates for NNs application are antenna systems because of their associated nonlinearities. A multilayer perceptron with single hidden layer is capable of approximating any smooth non-linear input-output mapping, provided that there are sufficient number of neurons in the hidden layer, to an arbitrary degree of accuracy. This is referred as universal approximation property. Radial Basis Function NNs (RBFNs) poses the universal approximation capability, which was proven by Park and Sandberg [3]-[4]. As an extension to this property, a property of best approximation is defined. The model that most closely approximates the generating function, by some defined distance measure, from given set of models, is said that poses the best approximating property. RBFNs poses this property [5], and that's why they were applied to antenna array direction of arrival estimation and beamforming [6]-[8].

In this paper we present an examples of RBFNs application for intelligent antenna array synthesis and also for Faraday Polarization Rotation (FPR) estimation in the ionosphere. Next section describes the RBFNs architecture, and in Section 3 some results are presented.

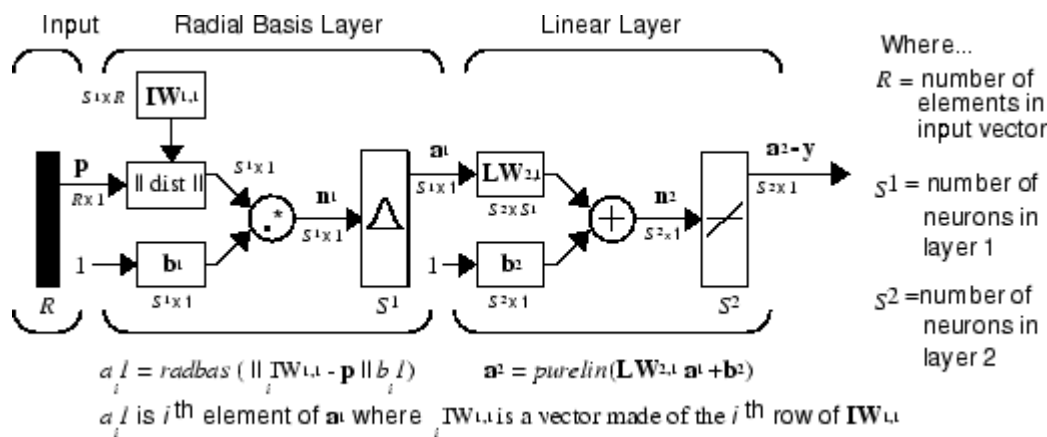


Fig.1 architecture of RBF NN

## 2. RBFN NN Architecture

Fig.1 [9] presents the architecture of RBF NN with two layers, one hidden and one output layer. The number of neurons in the hidden layer is  $S^1$  and the number of neurons in the output layer is  $S^2$ . The weighted input of the neuron is the weighted distance between the input vector and weight vector, and each net input of the neuron is dot product between that distance and bias vector. After passing through the *radbas* function the output of the hidden layer is generated, and that is actually the input vector for the second layer. The transfer function of the output layer is linear.

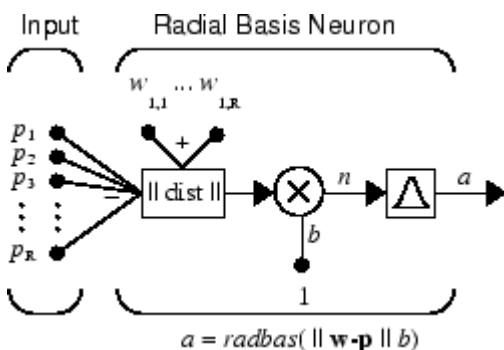


Fig. 2 RBF neuron architecture

Fig.2 [9] presents the structure of RBF neuron. Input vector has  $R$  elements, and output is presented with value  $a$ . The block *||dist||* presents some distance measure between the input vector and connection weights vector, and  $b$  presents the bias. At the end on the figure we can notice the block of the radial basis function as the activation function of the neuron. Radial basis transfer function block produce 1 whenever the input vector is matched with the weight vector which means it behaves as detector.

The input vector for antenna array synthesis is presented with limited number of values of array factor or radiation pattern, and the output presents the phase and amplitude step for the linear antenna array [10]-[11]. For faraday polarization rotation estimation, the input of RBF NN is latitude of the

monitored place and day time value, and the output is the total electron content [12]. NN has been used for different types of antennas [13]-[15], and here we discuss antenna array synthesis and faraday polarization rotation estimation with RBF NN.

## 3. Results

Array of elements placed along one direction are presenting the irregular linear antenna array, with different mutual distance among the neighbouring elements and with different amplitudes and phases among the excitations. The array factor in this case has the form:

$$F = \sum_{n=0}^M A_n e^{j\delta_n} \quad (1)$$

$$\delta_n = \beta d_n \cos\theta + \alpha_n \quad (2)$$

Where  $M+1$  is the number of antenna elements,  $A_n$  are the amplitudes of excitations,  $\beta$  is the phase constant ( $\beta=2\pi/\lambda$ ,  $\lambda$  is the wavelength),  $d_n$  are the mutual distances,  $\theta$  is the space angle and  $\alpha_n$  are the phase differences of the excitations. Even for modest number of antenna elements the array factor determination requires complex calculations for what we need to use computer calculations. Different distributions of mutual distances or mutual excitations among the elements produce variety of radiation patterns (array factors). Antenna array synthesis presents the determination of the parameters of the antenna array for already required radiation pattern or array factor.

In our analyses first we assume unit and uniform amplitude distribution where the inter-element distances is constant, and where the synthesis will be consisted of the phase difference determination between the neighbouring antenna elements. For this antenna array synthesis we assume regular linear antenna array where the radiation pattern is determined by the number of antenna elements  $M$ , mutual distance of the elements  $d$  and the phase difference  $\alpha$  between the two neighbouring elements. This simple structure will be a strong basis for further analyze

of irregular antenna arrays. The input of the NN is the radiation pattern vector and the output is the corresponding value of  $\alpha$  for given number of antenna elements and mutual distance.

The designing procedure for the RBE (Radial Basis with Exact solution) is outlined below.

The matrix P could be organized in R element vectors  $\mathbf{F}$ , which are presenting the radiation pattern in R points (Q vectors in total).

We have two steps:

1) Network designing

- 1) Form the input vectors  $\{\mathbf{F}^q, q=1,2, \dots, Q\}$ .
- 2) Generate input/output pairs  $\{\mathbf{F}^q, \alpha^q\}$ , where  $q=1,2, \dots, Q$ .
- 3) Design the RBE.

2) Network testing (Generalization)

- 1) Form the vectors  $\mathbf{F}'$  for the testing input samples.
- 2) Present input vectors  $\mathbf{F}'$  to the RBE.
- 3) Get the output of the network.

In the next step we assume linear amplitude distribution with parameter  $\Delta A$ . Again the phase difference between two neighbouring antenna elements is  $\alpha$ . In this case the array factor will be:

$$F = \sum_{n=0}^M (A_0 + n\Delta A) e^{jn\delta} \quad (3)$$

where

$$\delta = \beta d \cos\theta + \alpha \quad (4)$$

This time the output NN layer will have two neurons, one giving the value of  $\alpha$  and the other giving the value of  $\Delta A$ .

The designing procedure for the RBE is outlined below.

The matrix P could be organized in R element vectors  $\mathbf{F}$ , which are presenting the radiation pattern in R points (Q vectors in total).

We have two steps:

1) Network designing

- 1) Form the input vectors  $\{\mathbf{F}^q, q=1,2, \dots, Q\}$ .
- 2) Generate input/output pairs  $\{\mathbf{F}^q, \mathbf{t}^q\}$ , where  $q=1,2, \dots, Q$ , and  $\mathbf{t}$  is two element vector containing the  $\alpha$  and  $\Delta A$  value.
- 3) Design the RBE.

2) Network testing (Generalization)

- 1) Form the vectors  $\mathbf{F}'$  for the testing input samples.
- 2) Present input vectors  $\mathbf{F}'$  to the RBE .
- 3) Get the output of the network,  $\alpha$  and  $\Delta A$ .

The main goal is to observe the influence of additional parameter in the NN and that is parameter  $\Delta A$ , to the performance of the network. That will give us information for further inclusion of other parameters or different amplitude distributions, which finally would lead us to irregular array synthesis.

First we may consider regular linear array with uniform amplitude distribution. Fig.3 presents the antenna array factor for 9 antenna elements and with excitation phase difference of  $-44^\circ$  and  $44^\circ$ . The mutual distance between the elements is half wavelength. The training samples were picked with angle step (Alfa Step) of  $\alpha$  of  $0.5^\circ, 1^\circ, 1.5^\circ$ , and  $2^\circ$ , in the range  $(-45^\circ \div 45^\circ)$ . The input samples for the array factor were for angle step of  $0.25^\circ, 0.5^\circ, 1^\circ$ , and  $2^\circ$ . The testing samples were picked with step of  $0.05^\circ$ . The results for the mean error rate at the output of the NN are presented in Fig.4.

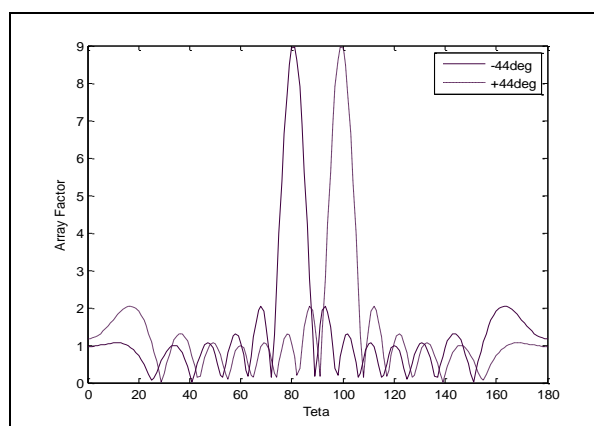


Fig.3 Array factor for M+1=9 and uniform amplitude distribution

Now we may consider linear amplitude distribution antenna array. Fig.5 presents the array factor for six antenna elements. For the experiment we fixed  $\alpha=45^\circ$  and we used training set for  $\Delta A=(0 \div 1)$  with steps 0.005; 0.01; and 0.02. The array factor input samples were chosen for angle step of  $1^\circ$ . The mutual element distance was one half wavelength. The mean error for  $\Delta A$  at the output of the RBE is presented on Fig. 6.

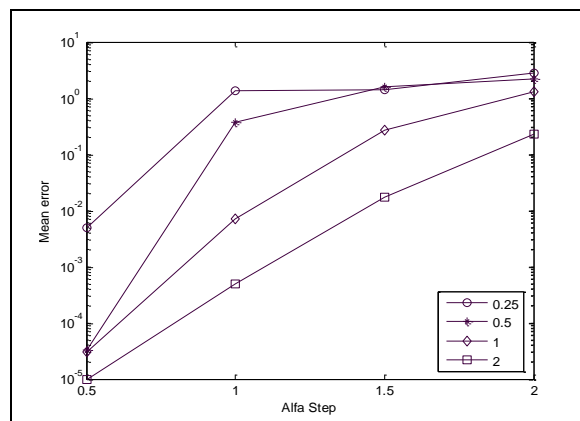


Fig.4 Mean error for M+1=9 and  $d=0.5\lambda$

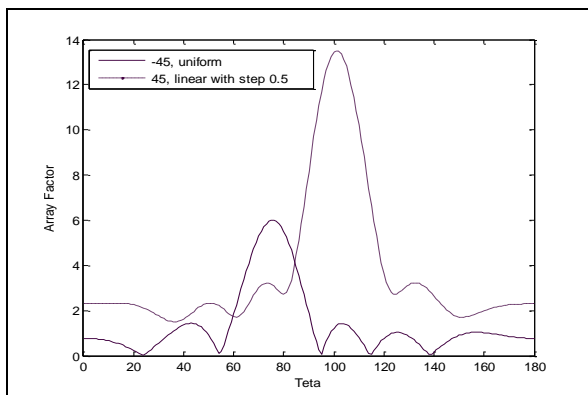


Fig.5 Array factor for  $M+1=6$ , uniform and linear amplitude distribution

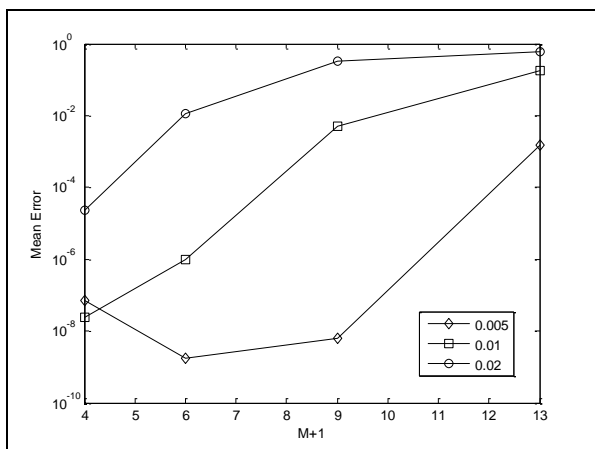


Fig.6 Mean error for  $\Delta A=(0\div 1)$  and  $\alpha=45^\circ$

Some of the results using RBF NN for Faraday Polarization Rotation (FPR) are presented in Fig.7 and Fig.8. We may notice a low mean error values and good match between the referent values and RBF NN values.

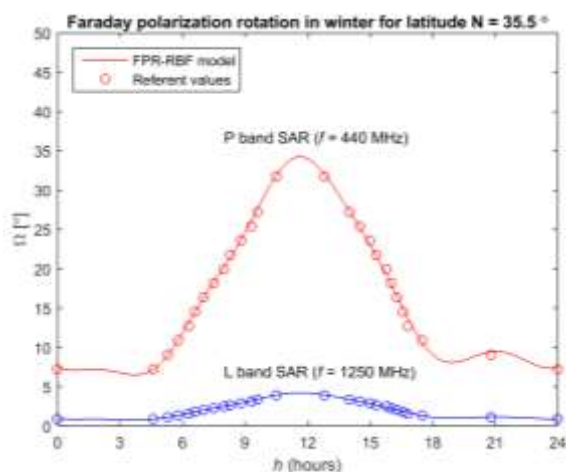


Fig. 7. Ionospheric FR angle of the P-SAR signal ( $f = 440$  MHz) and L-SAR signal ( $f = 1250$  MHz) obtained by FPR-RBF model

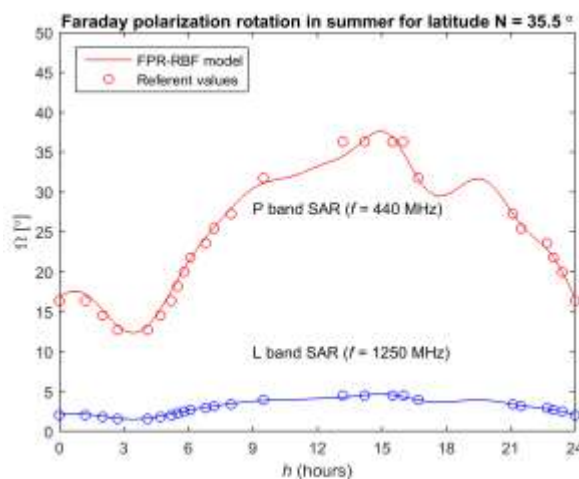


Fig. 8. Ionospheric FR angle of the P-SAR signal ( $f = 440$  MHz) and L-SAR signal ( $f = 1250$  MHz) obtained by FPR-RBF model

The FPR-RBF model was applied for FR angle estimation of the P-band SAR ( $f = 440$  MHz) and L-band SAR ( $f = 1250$  MHz) signals which propagate through the ionosphere above the Mediterranean area. Ionosphere FR angle of the P-SAR and L-SAR signals in 24h winter period for latitude  $la$  (N) =  $35.5^\circ$  and  $39.5^\circ$  obtained by FPR-RBF model are shown in Fig. 7 and Fig. 8 respectively. For each latitude with this model we generated the FR angle values for daytime period with resolution of 6 min which means 241 samples. The results gained with FPR-RBF model are compared to referent values on  $TEC$  (Total Electronic Content) values read from existing maps. We may observe a good match of the results gained with neural model with the referent values can be observed. The FR angle values of the P-SAR and L-SAR signals in 24 h summer period, obtained by FPR-RBF model, are shown in Fig. 9 and Fig. 10 for latitude  $la$  (N) =  $35.5^\circ$  and  $39.5^\circ$ , respectively. The same resolution of 6 min which means 241 points is used. Again we compare the results gained with neural model with referent values gained from existing maps. We may observe a good match with the referent values for the summer as in the case of winter. All results are generated for  $B_{//avg} = 26 \mu T$  belonging to the field change range valid for the Mediterranean area.  $B_{avg}$  is the average Earth's magnetic field intensity in T

The effect that influence the work on satellite communications systems especially for work of SAR systems in L and P band is Faraday Polarization Rotation of the EM wave in the ionosphere. That's why of great importance is the estimation of the angle of Faraday rotation in ionosphere for prediction and error correction in work of these systems caused by FPR. That's why the unavoidable task is to estimate the concentration of free electrons on a propagating path in ionosphere, or  $TEC$  value. Mainly we use empirical models of the vertical profile of the ionosphere to estimate  $TEC$  values today, that are gained based on large number of measured results gained with satellite systems or vertical sounding in longer time period. These models unavailable to ordinary users and are very complex. Alternative to these models based on

available measured data is to form neural network model for TEC values. It is proven that this model is easy to be realized and it can determine TEC values quickly based on space and time information of the signal propagation in the ionosphere. Previously shown results for used FPR\_RBF neural model for FR angle estimation for winter and summer period in the Mediterrean region provide good evidence that the use of NNs to solve this problem is a good choice. The results also prove that neural network models are a good alternative for the expensive and hardware demanding numerical models but also for software for description of the ionosphere influence on EM propagating waves. This models are also good alternative for slow and rough estimation of manual reading of TEC values.

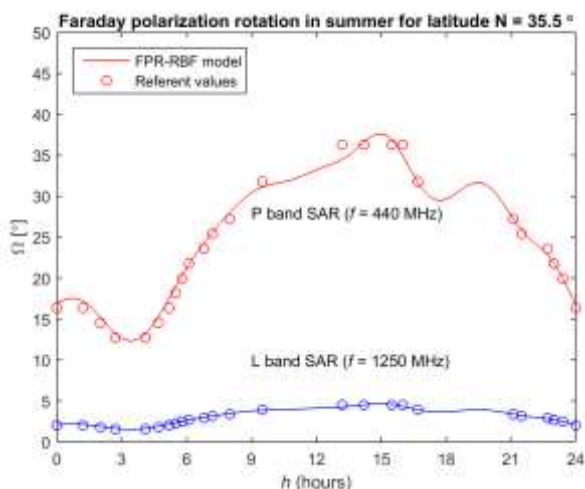


Fig. 9. Ionospheric FR angle of the P-SAR signal ( $f = 440$  MHz) and L-SAR signal ( $f = 1250$  MHz) obtained by FPR-RBF model

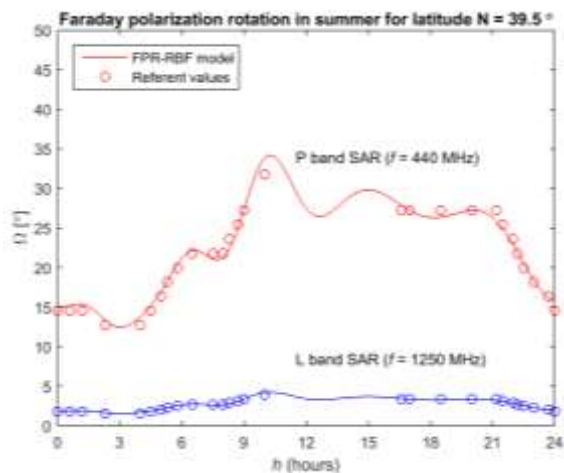


Fig. 10. Ionospheric FR angle of the P-SAR signal ( $f = 440$  MHz) and L-SAR signal ( $f = 1250$  MHz) obtained by FPR-RBF model

## References

[1] C.G. Christodoulou, and M. Georgiopoulos, “Application of Neural Networks in Electromagnetics”, Artech House, Inc., 2001.

[2] M. M. Gupta, L. Jin, and N. Homma, “Static and Dynamic Neural Networks”, A. John Wiley & Sons, Inc., Publication, 2003.

[3] Park, J., and I. W. Sandberg, “Approximation and Radial Basis Function Networks”, Neural Computation, Vol. 5, 1993, pp. 305-316.

[4] Park, J., and I. W. Sandberg, “Universal Approximation Using Radial Basis Function Networks”, Neural Computation, Vol. 3, 1991, pp. 246-257.

[5] Federico Girosi, and Tomaso Poggio, “Networks and the Best Approximation Property”, A.I. Memo No. 1164, C.B.I.P. Paper No.45, October 1989.

[6] M. Sarevska, B. Milovanović, and Z. Stanković, “Alternative Signal Detection For Neural Network-Based Smart Antenna”, IEEE Conf. NEUREL’04, Belgrade, Serbia, September 2004.

[7] Maja Sarevska, Bratislav Milovanović, and Zoran Stanković, “Reliability of Radial Basis Function – Neural Network Smart Antenna”, Conf.WSEAS’05 on Communications, Athens, Greece, July 2005.

[8] Maja Sarevska, “Signal Detection For Neural Network-Based Antenna Array”, Conf.NAUN’08 on Circuits, Systems, and Signals, Marathon, Attica, Greece, June 2008, pp.115-119.

[9] <https://www.mathworks.com/help/deeplearning/ug/radial-basis-neural-networks.html>

[10] Maja Sarevska, Nikos Mastorakis, ‘Regular Antenna Array Synthesis Using Neural Network’, 10th WSEAS Int. Conf. on TELECOMMUNICATIONS and INFORMATICS (TELE-INFO’11) 27-29 May, 2011, Lanzarote, Canary Islands, Spain.

[11] Maja Sarevska, Zoran Stanković and Bratislav Milovanović, “Antenna Array Synthesis for Triangle Amplitude Distribution”, Conf. ICIST 2012 - 2nd International Conference on Information Society Technology, Kopaonik, Serbia, March 2012, pp.200-204..

[12] Zoran Stankovic, Maja Sarevska, and Nebojsa Doncov, “Faraday Polarization Rotation in the Ionosphere Using Radial Basis Function ANN”, TELSIS, Nis, Serbia, October 20-22, 2021.

[13] Maja Sarevska, Zoran Stankovic, Nebojsa Doncov, Ivan Milovanovic and Bratislav Milovanovic, “Design of well-matched UHF Planar Bowtie Dipole Antenna using Neural Model”, TELSIS, Nis, Serbia, October 23-25, 2019.

[14] Zoran Stankovic, Nebojsa Doncov, Biljana Stosic, Maja Sarevska, and Ivan Milovanovic, “Design of well-matched Microwave Slot Antenna on a Flat Metal Grounded Plate using Neural Model”, Int. Sci. Conf. Icest’2020, Niš, September, 2020.

[15] Zoran Stankovic, Maja Sarevska, Nebojsa Doncov, and Ksenija Pesic “Planar Archimedean Spiral Antenna Resonant Frequency and Bandwidth Estimation using MLP Neural Network”, ETRAN, Novi Pazar, June, 2022, in preparation.

**Creative Commons Attribution License 4.0 (Attribution 4.0 International, CC BY 4.0)**

This article is published under the terms of the Creative Commons Attribution License 4.0

[https://creativecommons.org/licenses/by/4.0/deed.en\\_US](https://creativecommons.org/licenses/by/4.0/deed.en_US)